The International Journal of Engineering and Information Technology

journal homepage:www.ijeit.misuratau.edu.ly

Modeling of Opposing Mixed Convection of Air in Partially Cooled Vertical Channels

Musa M. Radwan
University of Tripoli, Faculty of Engineering
Tripoli / Libya
M.Radwan@uot.edu.ly

Abstract—**in this paper opposing laminar mixed convection in partially cooled vertical channel is investigated numerically. Temperature profiles, Nusselt number and velocity profiles at various axial locations in the cooled part of opposing buoyancy flow are presented. Streamlines and isotherms have been also plotted for different values of Grashof number, *Gr*. Conservation equations of continuity, momentum and energy were solved simultaneously using Finite volume method. The effect of the cooled section on the flow pattern and heat transfer performance is investigated for given Grashof numbers. The influence of axial diffusion and it's relevant to flow reversal at the entrance region of the channel was taken into account in the governing equations and particular attention is given to the ratio $|Gr / Re^2|$. The effect of opposing bouncy forces on the hydrodynamic and thermal fields was examined for air with Re = 500, $10^5 \leq |Gr \leq | 3*10^5$. Reversal flow was observed near the channel wall for this opposing buoyancy flow. It was noticed that the friction factor, $f \cdot Re_L$,for the ratio $|Gr / Re^2| \geq 1.2$ was unstable over the cooled length, becomes negative and then increases to an asymptotic value of 16 over the insulated section. The presented numerical results revealed some interesting features which may be summarized as: (i) Globally Nusselt number decreases and reaches asymptotic value at the end of the cooling section. However for *Gr* = $-3*10^5$ Nusselt decreases and reach a minimum value approximately equal to 3.12. (ii) For *Gr* up to $|3 \cdot 10^5|$ the Boussinesq approximation still predicts reasonably the heat transfer rate.**

Index Terms: **Mixed convection, Flow in Channel, Heat fluxes, Finite volume**

I. INTRODUCTION

The importance of mixed convection in ducts originates from its wide range of practical applications, including cooling of discrete heat sources mounted on electronic equipments, as well as the design of compact heat exchangers, solar collectors and cooling of voltaic cells. Numerous theoretical and experimental investigations concerning fluid flow in ducts of various shapes are available in the literature, Aung [1], Gebhart et al [2], Incropera [3] and Beijan [4]. Convection heat transfer may be classified according to the type of flow; heat is transferred by forced convection when external means such pumps or fans are used to pump a fluid over a solid surface. In contrast, natural or free convection occurs when the flow is induced by bouncy forces, due to density gradient as a result of temperature variation in the fluid. In addition, mixed convection, natural and forced may exist simultaneously if velocities associated with the forced flow are small and bouncy forces are large hence a secondary flow that is comparable to the imposed forced flow could be induced. Under this conditions the axial velocity may increase near the channel walls and decrease within the core region with possible existence of flow recirculation in the entry region for large bouncy forces [5, 6]. The effect of bouncy on heat transfer in a forced flow is strongly influenced by the direction of the bouncy force relative to that of the flow. These are (i) aiding (assisting flow), (ii) opposing flow, (iii) transverse flow, it is well known that heat transfer is enhanced by aiding and opposing flow but it is reduced for the transverse case. This work, considers the effect of thermal bouncy on the flow field commonly termed as opposing bouncy mixed convection. Recently, considerable research including numerical and analytical studies has been conducted [7, 9], in particular for flows in horizontal and vertical tubes. In these studies the Boussinesq approximation has been suggested and implemented, which is based on two aspects, first the physical properties of the fluid are assumed constant except for the density. Second, the density variation in the continuity equation is ignored, but it is expressed as a linear function of temperature in the bouncy terms [10].

In the last decades with the availability of high speed computing facilities, it has been possible to analyze the validity of the constant property assumption in modeling convection heat transfer problems [11]. The validity of Boussienq approximation has been investigated by Giorgini and Gray [12] where the case of natural convection for gases and liquids between two parallel isothermal surfaces has been investigated and the results of their study has revealed the validity of the Boussienq approximation for small temperature gradients. However,

Received 11 Dec, 2020; revised 27 Feb, 2021; accepted 28 Feb, 2021.

Available online 13 Mar, 2021.

for large temperature difference, the numerical solution become unstable and deviates from experimental data. Despite the fact that many works dealing with internal natural convection flow [13-16], relatively little work has been conducted to investigate the flow of air in partially cooled vertical channel with mixed convection. Few works found in the literature are those of Aung [17], who has solve numerically the momentum and energy equations for upward heated flow of an ideal gas inside a vertical concentric annulus. However, the validity of Boussienq approximation was not included in their model. Nesserdine [18] has investigated the variable property flow model of partially heated or cooled tube and compare the results with Boussienq approximation model; the results of the two models were very close for low to moderate Grashof number. In the present work, we have presented a model for opposing mixed convection flow of air in partially cooled vertical channel. Numerical results for flow and thermal fields are presented and the effect of the cooling section is investigated.

II. MATHEMATICAL MODEL

This work is concerned with developing mixed convection flow in the entrance region of a vertical channel; the physical model under consideration is illustrated in Figure 1. The channel wall is cooled over a finite length L_c/D_h and insulated elsewhere. The fluid enters the channel with uniform velocity and temperature. Simulations were performed for air as the working fluid and corresponding to the following $\mathbf{10^5 \le |\, Gr \,| \le 3*10^5}$, $L_c/D_h = 10$, Note that the insulated section of the channel is considered long enough, $L_{in}/D_h = 90$ to allow for fully devolved profiles , even for high Gr.

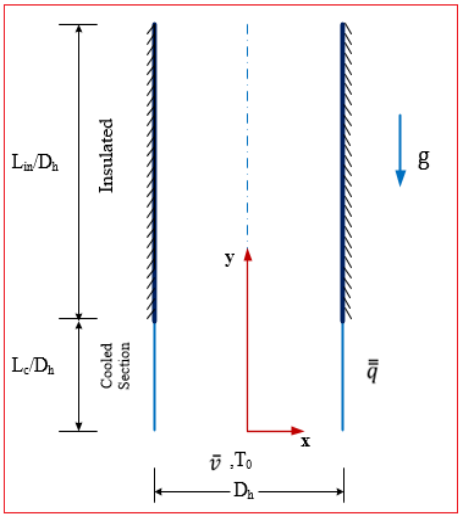

Figure 1. Schematic representation of the physical model.

The mathematical model of the problem is constructed taking into account the following simplifying assumptions:

- The flow is steady, laminar and two dimensional
- The flow is Incompressible and Newtonian.
- The viscous dissipation and compression work are neglected.

Based on the above mentioned assumptions, the governing equations of the flow were derived from the basic conservation principles of mass, momentum, and energy and can be written as [3,4]:

$$\frac{\partial(\rho u)}{\partial x}+\frac{\partial(\rho v)}{\partial y}=0 \tag{1}$$

$$\frac{\partial(\rho uu)}{\partial x}+\frac{\partial(\rho uv)}{\partial y}=-\frac{\partial p}{\partial x}+\mu\left[\frac{\partial^2 u}{\partial x^2}+\frac{\partial^2 u}{\partial y^2}\right] \tag{2}$$

$$\frac{\partial(\rho uv)}{\partial x}+\frac{\partial(\rho vv)}{\partial y}=-\frac{\partial p}{\partial y}+\mu\left[\frac{\partial^2 v}{\partial x^2}+\frac{\partial^2 v}{\partial y^2}\right]-\rho g\beta[T-T_0] \tag{3}$$

$$\frac{\partial(\rho uT)}{\partial x}+\frac{\partial(\rho vT)}{\partial y}=\Gamma\left[\frac{\partial^2 T}{\partial x^2}+\frac{\partial^2 T}{\partial y^2}\right],\ \Gamma=\frac{k}{c} \tag{4}$$

The associated boundary conditions for the above equations are [5]:

$$At\ x=0\ ;\quad \frac{\partial T}{\partial x}=0\quad ;\frac{\partial v}{\partial x}=0 \tag{5}$$

$$At\ \ x=\frac{D_h}{2};\quad u=v=0 \tag{6}$$

$$At\ y=0\,;u=0\,;v=\bar{v}\,;T=T_0 \tag{7}$$

$$At\ 0\le y\le L_c\ ;q''=\ -k\frac{\partial T}{\partial x} \tag{8}$$

$$At\ L_c\le y\le L_{in}\ ;k\frac{\partial T}{\partial x}=0 \tag{9}$$

$$At\ y=y_L;\frac{\partial u}{\partial y}=\frac{\partial v}{\partial y}=\frac{\partial T}{\partial y}=0 \tag{10}$$

Equation (7) prescribe a uniform velocity and a uniform temperature at the channel entrance, and equation (10) assumes the stream wise energy diffusion flux to be negligible and fully developed velocity profiles at the outlet.

Friction Factor and Nusselt Number

The definitions of two physical parameters of practical importance are introduced here. The first is the friction factor f , which is given by the following expression [3]

$$f=-\frac{2}{\mathrm{Re}_L}\left(\frac{\partial v}{\partial x}\right)_{x=D_h/2} \tag{11}$$

Where Re_L is the local Reynolds number defined as

$$\mathrm{Re}_L=\frac{\rho\bar{v}D_h}{\mu} \tag{12}$$

The second parameter of interest is the local Nusselt number, defined as [3]:

$$Nu_L=\frac{q''D_h}{k(T_w-T_b)} \tag{13}$$

Were the bulk temperature, T_b, is defined as [4]:

$$T_b = \frac{\int_0^{D_h/2} \rho C_p v T dx}{\int_0^{D_h/2} \rho C_p v dx} \quad (14)$$

The above equations are put in dimensionless form by defining the following dimensionless variables:

$$X = \frac{x}{D_h} \quad ; \quad Y = \frac{y}{D_h} \quad ; \quad U = \frac{u}{\bar{v}} \quad ; \quad V = \frac{v}{\bar{v}} \quad (15)$$

$$\theta = \frac{T - T_0}{q'' \frac{D_h}{k}} \quad ; \quad P = \frac{p + p_0}{\rho_0 \bar{v}^2} \quad (16)$$

Using the above defined variables, the governing equations can be casted in dimensionless form as:

$$\frac{\partial(U)}{\partial X} + \frac{\partial(V)}{\partial Y} = 0 \quad (17)$$

$$\frac{\partial(UU)}{\partial X} + \frac{\partial(UV)}{\partial Y} = -\frac{\partial P}{\partial X} + \frac{1}{\mathrm{Re}}\left[\frac{\partial^2 U}{\partial X^2} + \frac{\partial^2 U}{\partial Y^2}\right] \quad (18)$$

$$\frac{\partial(UV)}{\partial X} + \frac{\partial(VV)}{\partial Y} = -\frac{\partial P}{\partial Y} + \frac{1}{\mathrm{Re}}\left[\frac{\partial^2 V}{\partial X^2} + \frac{\partial^2 V}{\partial Y^2}\right] - \frac{Gr}{\mathrm{Re}^2}\theta \quad (19)$$

$$\frac{\partial(U\theta)}{\partial X} + \frac{\partial(V\theta)}{\partial Y} = \frac{1}{\mathrm{Pr}\,\mathrm{Re}}\left[\frac{\partial^2 \theta}{\partial X^2} + \frac{\partial^2 \theta}{\partial Y^2}\right] \quad (20)$$

The dimensionless form of the boundary conditions can be written as:

$$At\ x = 0; \frac{\partial \theta}{\partial X} = 0; At\ x = 1; U = V = 0 \quad (21)$$

$$At\ Y = 0\ V = 1 \quad ; \quad \theta = 0 \quad (22)$$

$$0 \le Y \le \frac{L_c}{D_h}; \frac{\partial \theta}{\partial X} = 1 \quad (23)$$

$$\frac{L_c}{D_h} \le Y \le \frac{L_{in}}{D_h}; \frac{\partial \theta}{\partial X} = 0 \quad (24)$$

$$At\ Y = Y_L; \frac{\partial U}{\partial Y} = \frac{\partial V}{\partial Y} = \frac{\partial \theta}{\partial Y} = 0 \quad (25)$$

Friction factor and Nusslet number, equations (11, 13) can be written as:

$$f = -\frac{2}{\mathrm{Re}_L}\left(\frac{\partial V}{\partial X}\right)_{X=1} \quad ; \quad Nu_L = \frac{1}{(\theta_w - \theta_b)} \quad (26)$$

III. NUMERICAL SOLUTION

The solution of the conservation equations of mass, momentum and energy is obtained by expressing the dimensionless form of these equations and the associated boundary conditions in a discrete form using finite volume method [1] and the simple procedure is adopted for the linkage of velocities and pressure through the continuity equation. In this method, the computational domain is divided into a number of non-overlapping control volumes, where pressure and temperature are stored at the center of each cell, while the velocity components, u and v are stored at the control volume faces (staggered grid) to avoid checkerboard pressure field [19]. The governing equations were discretized to produces a set of linear algebraic equations which are solved simultaneously with the tridiagonal matrix algorithm (TDMA). The line by line method has been used where the domain is covered by a number of sweeps in the x- and y directions. A uniform mesh is employed in both the axial and transverse directions and sufficient grid distribution was used to ensure that results are independence of mesh size. Figure 2 shows the results of the friction factor for different mesh size and 50 by 500 grid distribution was found optimum for acceptable results. The mass source residual, R, which is defined as the sum of the absolute values of the net mass fluxes into and out of every control volume is used as convergence criterion. The code stops if the mass source residual falls below 10^{-6}. The converged solution for forced convection was checked against the exact solution of the velocity profile at the channel out let (parabolic) a good agreement was noticed.

IV. RESULTS AND DISCUSSION

As mentioned previously, the objective of this work is to determine the combined effects of mixed convection on hydrodynamic and thermal fields for partially cooled vertical channels; this was achieved by computing velocity and temperature profiles, friction factor and Nusselt number. Isotherms and streamlines were plotted for different values of Grashof number. It is worth mentioning here that the results of the present study were for the range of $10^5 \le |Gr| \le 3*10^5$; Re = 500, Pr = 0.7 and $L_c/D_h = 10$. Note that in order to achieve parabolic profiles for velocity and temperature, the length of the insulated section is kept as $L_{in}/D_h = 90$ for all simulations.

A Grid-independence

For the purpose of grid independence test, the values of Re and $|Gr|$ for mixed convection were chosen as 500 and 10^5 respectively. Grid independence is established by monitoring the friction factor values for different grid sizes. In choosing the optimum mesh for the converged results, the number of control volumes for successive grids were increased roughly by a factor of 1.5 in each direction. The results of the grid variation study are presented in Figure 2, based on these results a mesh of 50 control volume in the x- direction by 500 control volume in the y- direction was adopted for the rest of numerical calculations.

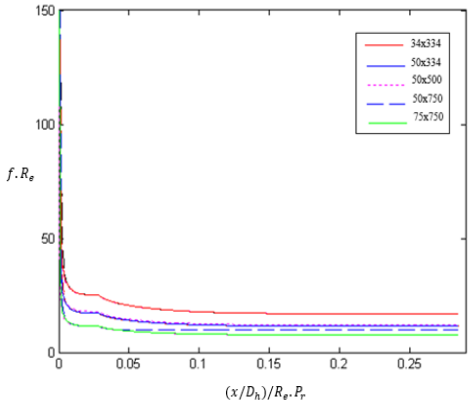

Figure 2. Friction factor values for different grid sizes

B *Flow Field and Friction Factor*

It is evident from Figure. 3, Figure. 4, and Figure. 5 that the dimensionless axial velocity, v, is zero at the wall due to no-slip condition. In addition, these Figures display the axial velocity profile in the cooled part of the channel for opposing buoyancy flow, and show the axial velocity distribution at three axial positions for different values of Grashof numbers that represent the ratio of the bouncy forces to the viscous forces. For the given range of Grashof number, the velocity distributions deviates from the forced convection case, except at low value of *Gr*, where the shape of the velocity curve far enough from the entrance is equivalent to the fully developed channel flow; this is shown in Fig. 3. However, at moderate values of Grashof number where the combined effects of natural and forced convection contribute equally to the flow, the velocity distribution at the same axial location deviates from the fully developed case. This is shown in Fig. 4, as can be seen, the velocity increases at the centerline of the channel, and at some location near the wall, X = 0.4, it drops to 0.28 for *Gr* = -2*10^5 compared to v = 0.5 at the same location for *Gr* = -10^5 and approaching zero exactly at the channel wall. Fig. 5 demonstrates clearly the departure from the pure forced convection case and shows the effect of natural convection on the flow field. In this figure, the dimensionless axial velocity at the center of the channel increases to its maximum value of 1.8, while it is approaching negative value of -0.06 near the wall, thus one may expect that, this value of critical *Gr* corresponding to the onset of the reverse flow. It is very interesting to observe that the Boussinesq approximation underestimates systematically the fluid axial velocity near the channel wall but it was overestimated at the center of the channel. This effect is negligible in the vicinity of the inlet section, where the fluid temperature is not affected yet by the cool walls. The underestimation of the velocity values increases considerably with the increase of $|Gr|$, as shown in Fig. 5 for $|Gr|$ = 3*10^5 and L_c/D_h =10.

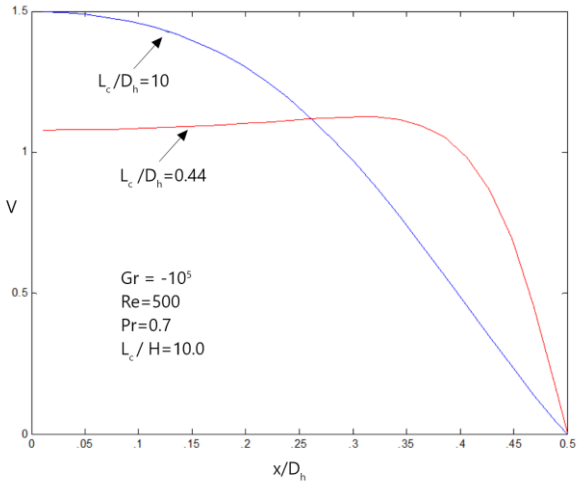

Figure 3. Axial velocity profiles for Gr = -10^5

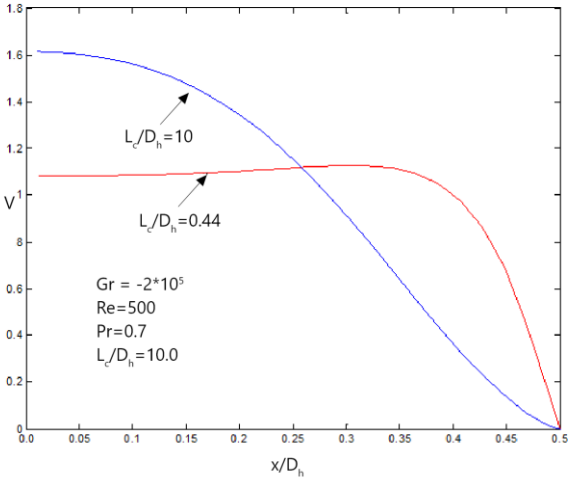

Figure 4. Axial velocity profiles for Gr = -2* 10^5

Figure. 5 also shows that the hydrodynamic field is different from that corresponding to pure forced Convection. As the fluid moves downstream, the distortion of the velocity profile becomes larger, as expected; the acceleration of the fluid particles near the center of the channel is compensated by deceleration near the wall of the channel. Seeing that *Gr*/Re^2 is bigger than unity in this case (i.e. the inertia forces less important than the buoyancy forces), the deceleration causes a reversal flow characterized by a negative axial velocity near the wall of the channel.

Figure 6 shows the streamlines plot for different values of *Gr*. It is interesting to mention that the flow reversal starts to develop at the end of the cooled section and near the wall. It should be noted that, the reverse flow does not exist for low value of *Gr* as shown in Fig. 6a where forced convection dominates the flow, but the recirculation zone starts to develop as the value of $|Gr|$ increased to a certain value where both natural and forced convection effects have considerable effect. This is shown in Fig. 6b, where the reverse flow starts to originate as the fluid exits the cool region of the channel.

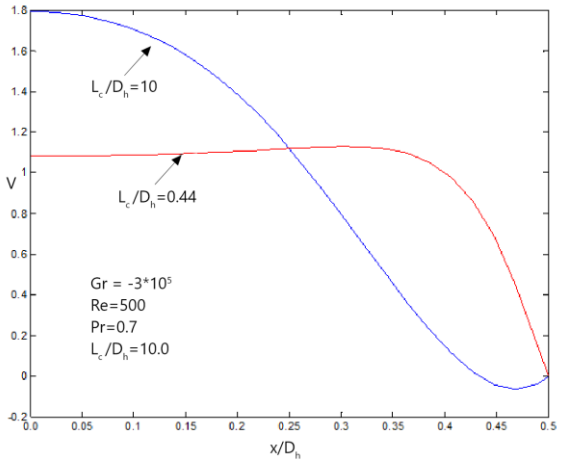

Figure 5. Axial velocity profiles for Gr = -3*10^5

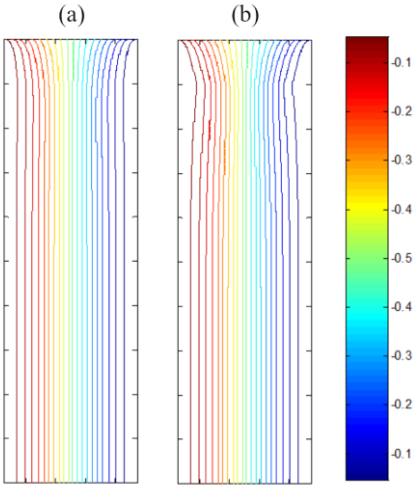

Figure 6. Streamlines for (a) Gr = -10^5, (b) Gr = -3*10^5.

Figure. 7 shows the axial evolution of the product *f•Re* for the opposing flow. Since the friction factor is directly related to the velocity gradient on the channel wall, equation (11), a minimum value of this product occurs at the end of the cooling section for each value of *Gr*, where the flow reversal starts and increases to attain its constant value far downstream in the insulated section. As was mentioned earlier that the velocity profile in the channel was distorted as the ratio $\left| Gr/\mathrm{Re}^2 \right|$ increases, the fluid shear at the no-slip surface also change, since shear is caused by the velocity gradient, the shear will decrease at the cooled wall and due to mass conservation increase at the adiabatic boundary.

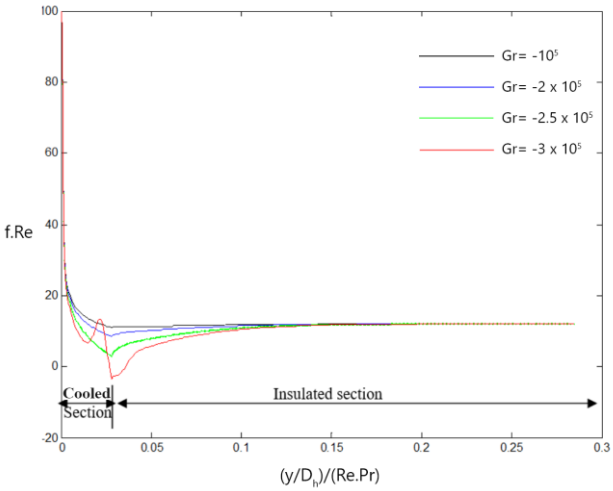

Figure 7. Local friction factors for opposing buoyancy.

C *Thermal Field and Nusselt number*

The temperature profiles at two specific axial locations are shown in Figure. 8, Figure. 9, and Figure 10. As can be seen, these profiles near the channel inlet are almost identical, independent of *Gr*. However, far down stream near the end of the cooling section they exhibit quasi parabolic shape but not yet fully developed. The dimensionless air temperature increases as the air moves from the entrance region to y/D_h = 10, this increase is higher near the wall and lower at the centerline, indicating that the flow is not thermally developed.

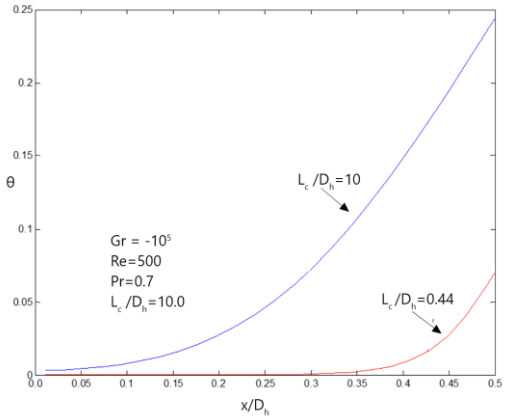

Figure 8. Temperature profiles for Gr = -10^5.

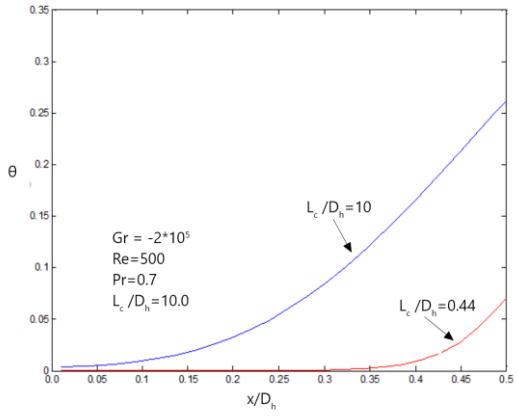

Figure 9. Temperature profiles for Gr = -2*10^5.

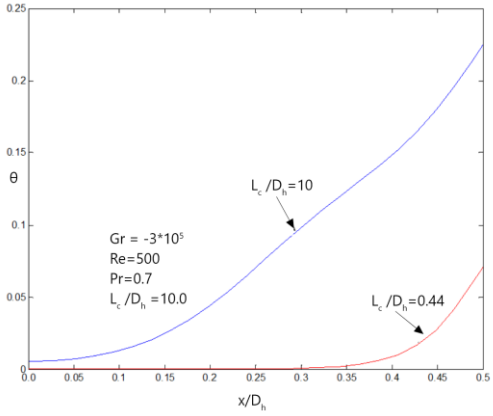

Figure 10. Temperature profiles for Gr = -3*10^5.

The dependency of temperature distribution on Gr is clearly demonstrated by Figure. 10 for Gr = -3*10^5 where the lack of smoothness is noticed, compared to Fig. 8 and Figure9 for lower value of $|Gr|$. This perturbation is due to the existence of recirculation zone on the temperature field near the channel wall. The recirculation zone has been predicted only for higher values of $|Gr|$ where bouncy driven effects are pronounced.

Figure. 11a, and Figure1b, both show the isotherms within the active heat transfer length at different values of Grashof numbers, G*r*. As can be seen, the contours are affected by the dimensionless parameter, Gr, and shows that the temperature is higher downstream which is maximum near the wall and decreasing toward the center of the channel. These Figures demonstrate the existence of vortices near the end of the cooling section; these are attributed to flow reversal where the velocity is very small and heat transfer takes place only by conduction.

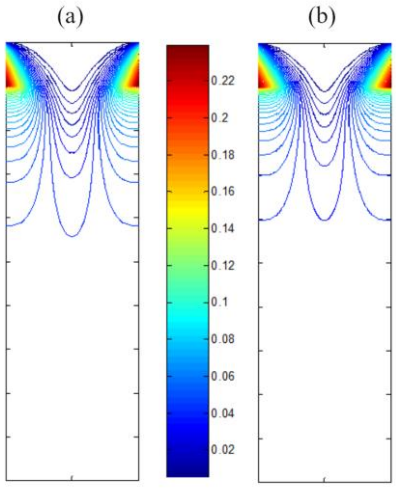

Figure 11. Isotherms for (a) Gr = -10^5 , (b) Gr = -3*10^5.

Finally, Figure. 12 shows the axial variation of the local Nusselt number. As can be seen for all values of Gr, Nusselt decreases and reaches asymptotic value at the end of the cooling section. However for Gr = -3*10^5 Nusselt decreases and reach a minimum value approximately equal to 3.12 that corresponds to the location of boundary layer separation, near this point the air velocity is very low which leads to heat transfer by conduction. The separation point is surrounded by a region of reverse flow where the bouncy forces oppose the flow. Beyond the separation point, Nusselt starts to increase and reaches the asymptotic value at the end of the cooling section.

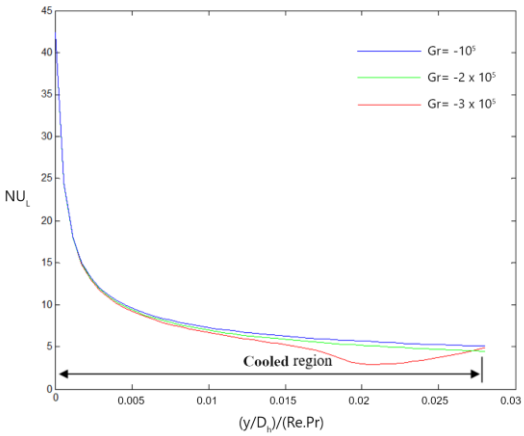

Figure 12. The axial evolution of the local Nusselt number for various Grashof numbers.

V. CONCLUSION

In this study, a comprehensive analysis of opposed laminar mixed convection in a two dimensional rectangular channel subjected to uniform cooling at the lower part of the wall has been carried out numerically. The governing equations were solved using the finite volume method. The results revealed that the flow structure, temperature distribution and heat transfer were strongly dependent on the absolute value of the ratio Gr / Re^2. It was found that for opposed buoyancy driven flow,

velocity and thermal maps are much more perturbed with the presence of recirculation cells close the cooled wall with increasing Gr/R_e^2 in absolute value. The effect of opposing bouncy forces on the hydrodynamic and thermal fields has been demonstrated for air with Re = 500, $0.4 \leq \left| Gr/Re^2 \right| \leq 1.2$ and Pr = 0.7. The numerical results presented, revealed some interesting features which may be summarized as:

1. Globally Nusselt number decreases and reaches asymptotic value at the end of the cooling section.
2. For Gr = -3*10^5 Nusselt decreases and reach a minimum value approximately equal to 3.12 that corresponds to the location of boundary layer separation, Beyond this point, Nusselt starts to increase and reaches the asymptotic value at the end of the cooling section..
3. For Gr up to -3×10^5 The Boussinesq approximation still predicts reasonably the heat transfer rate.
4. In general the cooled section modifies the flow field and hence the wall convective heat transfer.

REFRENCES

[1.] Aung, W., Moghadam, H.E., "*Simultaneous Hydrodynamic and thermal developing in mixed convection in a vertical annulus with fluid property variations*", Trans ASME, J. Heat transfer Vol 113, 1989, 926-930.

[2.] Gebhart, B., Jaluria, Y., Mahajan, R. et Sammakia B., "*Buoyancy-induced flows and transport*" New York, Hemisphere Publishing, 1988.

[3.] Incropera, Frank, P., DeWitt, David, P., "*Fundamentals of Heat and Mass Transfer", 6th ed, John Wiley 2007.*

[4.] *Bejan, A., "*Convection heat transfer", 3th ed. John Wiley & Sons Inc, 2004.

[5.] Desrayaud, G., Lauriat, G. "*Flow reversal of laminar mixed convection in the entry region of symmetrically heated, vertical plate channels*", International Journal of Thermal Sciences, 48(11), 2009, 2036–2045.

[6.] Laaroussi, N., Lauriat, G., Desrayaud, G. "*Effects of variable density for film evaporation on laminar mixed convection in a vertical channel*", International Journal of Heat and mass Transfer, 52(1), 2009, 151–164.

[7.] Patankar, S. V.,"*Numerical Heat Transfer and Fluid Flow*", McGraw-Hill, 1980.

[8.] Elenbaas, W., "*Heat dissipation of parallel plates by free convection*", Physica 9 1942, 1–28.

[9.] Dehghan, A. A., Behnia, M., "*Combined natural convection–conduction and radiation heat transfer in a discretely heated open cavity*", ASME J. Heat Transfer Vol 118, 1996, 56–64.

[10.] Chen, T., Armaly, B Aung, W., "*Natural Convection: Fundamentals and Applications*", 1985, 669–725.

[11.] Anand, N.K., Kim, S.H., Aung, W., "*Effect of wall conduction on free convection between asymmetrically heated vertical plates: uniform wall temperature*", Int. J. Heat Mass Transfer Vol 33, 1990, 1025–1028.

[12.] Kim, S.Y., Sung, H.J., Hyun, J.M., "*Mixed convection from multiple layered boards with cross-stream wise periodic boundary conditions*", Int. J. Heat Mass Transfer 35 (11), 1992, 2941–2952.

[13.] Rao, G. M., Narasimham, G.S., "Laminar conjugate mixed convection in a vertical channel with heat generating components". International Journal of Heat and Mass Transfer Vol 50, 2007, 3561–3574.

[14.] Aung, W., Moghadam, H. E., "Simultaneous Hydrodynamic and thermal developing in mixed convection in a vertical annulus with fluid property variations", Trans ASME, J. Heat transfer Vol 113, 1989, 926-930.

[15.] Braaten, M. E., Patankar, S. V., "Analysis of laminar mixed convection in shrouded arrays of heated blocks, International Journal of Heat and Mass Transfer", 28 (9), 1985, 1699–1709.

[16.] Tu¨rkolu, H., Yu¨N., cel, "Mixed convection in vertical channels with a discrete heat source", Heat and Mass Transfer Vol 30, 1995, 159–166.

[17.] Wang, Y., Vafai, K., "Heat transfer and pressure loss characterization in a channel with discrete flush-mounted and protruding heat sources", Experimental Heat Transfer Vol 12, 1999, 1–16.

[18.] Nesreddine, H., Galanis, N., "Recirculating flow in aiding/ opposing mixed convection in vertical pipes", Numerical Heat Transfer, Part A, 1997, 575-585.

[19.] Hornbeck, R. W., "An All- Numerical method for heat transfer in the inlet of a tube", ASME, 1965, Paper 65- WA/HT-36.

[20.] Z. Li, Z Huang, W.Tao., "The three dimensional numerical study in turbulent mixed convection", Energy procedia., Vol 75, 2015, 462-466

[21.] M.C. Moghadam, M.Edalatpour, J.P.Solano, "Numerical study on conjugated laminar mixed convection., J. Solar Energy, Vol 139 (4), 2019.

Nomenclatures

A	flow cross section area (m^2)
C	specific heat(kJ/kg.K)
f	friction factor
Gr	Grashof number based on heat flux
D_h	hydraulic diameter of the channel (m)
h	heat transfer coefficient
L_c	length of the cooling section (m)
L_{in}	length of the insulated section (m)
Nu_L	local Nusselt number
p	pressure (kPa)
P	dimensionless pressure
P_e	Peclet number,$R_e P_r$
P_r	Prandtl number
$\overline{\overline{q}}$	heat flux at the wall (W/m^2)
Re	Reynolds number
T	temperature
T_w	wall temperature
T_b	bulk temperature
u	velocity components in x-direction (m/s)
v	velocity components in y-direction (m/s)
U	dimensionless Velocity in x-direction
V	dimensionless Velocity in y-direction
$\overline{v}$	mean velocity (m/s)
x, y	Cartesian coordinates

Greek symbols

β	thermal expansion coefficient (K^{-1})
k	thermal conductivity (W/$m.k$)
θ	dimension less temperature
μ	dynamic viscosity ($Pa.\sec$)
v	kinematic viscosity (m^2/sec)
ρ	density (kg/m^3)
α	thermal diffusivity (m^2/sec)

Subscript

0	evaluated at the inlet temperature